Reprinted from June 1989, Vol. 111, Journal of Applied Mechanics

Kinking of a Crack Out of an Interface

Ming-Yuan He
Institute of Mechanics,
Chinese Academy of Sciences,
Beijing, China

John W. Hutchinson
Division of Applied Sciences,
Harvard University,
Cambridge, MA 02138
Fellow ASME

Kinking of a plane strain crack out of the interface between two dissimilar isotropic elastic solids is analyzed. The focus is on the initiation of kinking and thus the segment of the crack leaving the interface is imagined to be short compared to the segment in the interface. Accordingly, the analysis provides the stress intensity factors and energy release rate of the kinked crack in terms of the corresponding quantities for the interface crack prior to kinking. Roughly speaking, the energy release rate is enhanced if the crack heads into the more compliant material and is diminished if it kinks into the stiff material. The results suggest a tendency for a crack to be trapped in the interface irrespective of the loading when the compliant material is tough and the stiff material is at least as tough as the interface.

1 Introduction and Form of the Solution

A fracture mechanics of interfacial separation is beginning to emerge, although there are still conceptual difficulties to be overcome associated wtih the nonstandard oscillatory square root singularity of some interface cracks. In this paper an analysis of a crack kinking out of an interface is carried out with the aim of providing the crack mechanics needed to assess whether an interface crack will tend to propagate in the interface or whether it will advance by kinking out of the interface. The geometry analyzed is shown in Fig. 1. The parent interface crack lies on the interface between two semi-infinite blocks of isotropic elastic solids with differing elastic moduli. A straight crack segment of length a and angle ω (positive clockwise) kinks downward into material 2. The length a is assumed to be small compared to the length of the parent interface segment of the crack, and thus the asymptotic problem for the semi-infinite parent crack is analyzed. The stress field prior to kinking ($a \to 0$) is therefore the singularity field of an interface crack characterized by a complex intensity factor, $K = K_1 + iK_2$, to be specified precisely. The crack tip field at the end of the kinked crack is characterized by a combination of the standard mode I and mode II stress intensity factors, K_I and K_{II}. The analysis provides the relationships among K_1 and K_{II} for the kinked crack and K_1 and K_2 for the interface crack as dependent on the kink angle ω and the material moduli. The energy release rate of the kinked crack is also related to the energy release rate of the interface crack. Limiting results for the case when the moduli differences across the interface disappear are compared with previously published work on kinked cracks.

The remainder of this section is used to completely specify the functional form of the relationships sought. The numerical analysis is given in the next section and results and discussion are given in Sections 3 and 4. Section 2 containing the analysis may be skipped if one is primarily interested in the results.

Although there are three independent nondimensional material moduli parameters, Dundurs (1969) has shown that for problems of this class the solution depends on only two special parameters which in plane strain are

$$\alpha = [G_1(1-\nu_2) - G_2(1-\nu_1)]/[G_1(1-\nu_2) + G_2(1-\nu_1)] \quad (1)$$

$$\beta = \frac{1}{2}[G_1(1-2\nu_2) - G_2(1-2\nu_1)] / [G_1(1-\nu_2) + G_2(1-\nu_1)] \quad (2)$$

where G and ν are the shear modulus and Poisson's ratio and the subscript identifies the material as indicated in Fig. 1. Both α and β vanish when the dissimilarity between the elastic properties of the two materials vanishes and they change sign when the materials are interchanged.

The stress field for the semi-infinite interface crack ($a = 0$) has the form

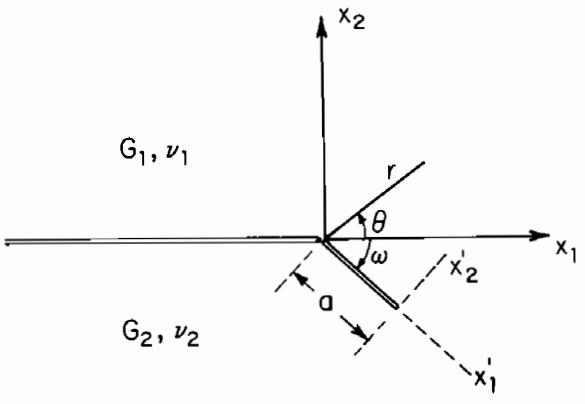

Fig. 1 Geometry of kinked crack

Contributed by the Applied Mechanics Division of THE AMERICAN SOCIETY OF MECHANICAL ENGINEERS for publication in the JOURNAL OF APPLIED MECHANICS.

Discussion on this paper should be addressed to the Editorial Department, ASME, United Engineering Center, 345 East 47th Street, New York, N.Y. 10017, and will be accepted until two months after final publication of the paper itself in the JOURNAL OF APPLIED MECHANICS. Manuscript received by ASME Applied Mechanics Division, March 7, 1988; final revision, September 1, 1988.

$$\sigma_{\alpha\beta} = Re\{K(2\pi r)^{-1/2} r^{i\epsilon} \tilde{\sigma}_{\alpha\beta}(\theta)\} \tag{3}$$

where $i = \sqrt{-1}$, r and θ are planar-polar coordinates centered at the origin, $K = K_1 + iK_2$ is the complex interface stress intensity factor, and

$$\epsilon = \frac{1}{2\pi} \ln\left(\frac{1-\beta}{1+\beta}\right). \tag{4}$$

The angular dependence $\tilde{\sigma}_{\alpha\beta}(\theta)$ is complex in general, but universal for a given material pair. On the interface ahead of the tip the tractions are

$$\sigma_{22} + i\sigma_{12} = K(2\pi r)^{-1/2} r^{i\epsilon}. \tag{5}$$

The notation and normalizations for the interface crack used here follow those introduced by Rice (1987) and Hutchinson, Mear, and Rice (1987) which, in turn, are based on the early papers on the subject by England (1965), Erdogan (1965), and Rice and Sih (1965). The interface intensity factors are defined so that $K_1 \to K_I$ and $K_2 \to K_{II}$ when the dissimilarity between the elasticity of the two materials vanishes. Note also that when $\beta = 0$ and thus $\epsilon = 0$, K_1 measures the normal component of the traction singularity acting on the interface while K_2 measures the shear component with the standard definitions for an intensity factor.

The complex interface factor $K = K_1 + iK_2$ is taken as the prescribed loading parameter in the present study. For a specific interface crack problem, K will necessarily have the dimensional form

$$K \equiv K_1 + iK_2 = (\text{applied stress}) \cdot L^{1/2} L^{-i\epsilon} F \tag{6}$$

which follows from its definition in equation (5), where L is a length quantity such as crack length or ligament length and F is a dimensionless function of the in-plane geometry and material moduli. Examples of specific solutions for K can be found in the aforementioned references.

The singular field at the tip of the kinked crack in material 2 is the classical field with conventional stress intensity factors K_I and K_{II} such that

$$\sigma_{2'2'} + i\sigma_{1'2'} = (K_I + iK_{II})(2\pi x_1')^{-1/2} \tag{7}$$

on the line ahead of the tip ($x_1' > 0$, $x_2' = 0$).

As already stated, the problem considered is the asymptotic one where a is small compared to all relevant in-plane length quantities (in particular, compared to L) so that the interface crack is taken as semi-infinite with stresses which remotely asymptote to (3). The relationship between the intensity factors of the kinked crack and the prescribed complex interface intensity K specifying the remote field can be written as

$$K_I + iK_{II} = c(\omega,\alpha,\beta) K a^{i\epsilon} + \bar{d}(\omega,\alpha,\beta) \bar{K} a^{-i\epsilon} \tag{8}$$

where ($\bar{}$) denotes complex conjugation and c and d are complex-valued functions of ω, α, and β.[1] The argument justifying (8) is as follows: The factors K_I and K_{II} have dimensions of stress • (length)$^{1/2}$ while K has the form (6). By dimensional considerations, a must combine with K as $Ka^{i\epsilon}$ or its conjugate, since in the asymptotic problem a is the only length quantity other than the length quantities implicit in K in (6). Equation (8) is a general representation of $K_I + iK_{II}$ consistent with this observation and with linearity. Use of $\bar{d}$ in (8) (rather than d) is purely for convenience. When $\epsilon = 0$, as when the material dissimilarity vanishes, or just when $\beta = 0$, the real and imaginary parts of (8) become

$$K_I = (c_R + d_R) K_I - (c_I + d_I) K_2 \tag{9}$$

$$K_{II} = (c_I - d_I) K_I + (c_R - d_R) K_2 \tag{10}$$

where $c = c_R + ic_I$ and $d = d_R + id_I$. This form is equivalent to that employed by Bilby, Cardew, and Howard (1977) and Hayashi and Nemat-Nasser (1981) in reporting results for the homogeneous kinked crack problems which will be discussed in Section 2.

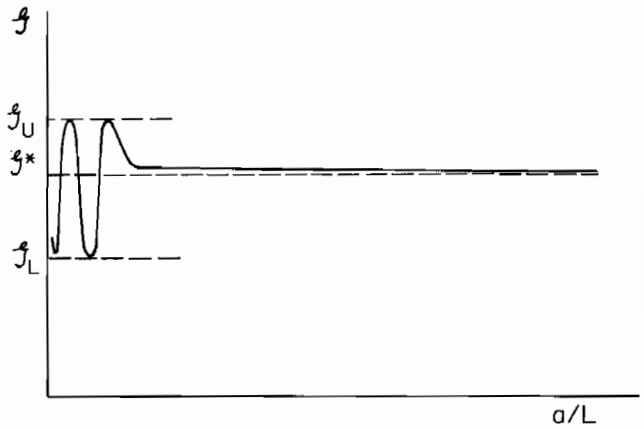

Fig. 2 Schematic variation of energy release rate with length of kinked segment of crack for $\beta \neq 0$

In plane strain, the energy release rate $\mathcal{G}_0$ of the interface crack advancing in the interface is related to K by (Malyshev and Salganik, 1965)

$$\mathcal{G}_0 = [(1-\nu_1)/G_1 + (1-\nu_2)/G_2] K\bar{K}/(4\cosh^2 \pi\epsilon) \tag{11}$$

in the new normalization. The energy release rate $\mathcal{G}$ of the kinked crack ($a > 0$) is given by

$$\mathcal{G} = [(1-\nu_2)/(2G_2)](K_I^2 + K_{II}^2). \tag{12}$$

By (8),

$$\mathcal{G} = [(1-\nu_2)/(2G_2)]\{(|c|^2 + |d|^2) K\bar{K} + 2R_e(cdK^2 a^{2i\epsilon})\}. \tag{13}$$

To reduce this expression further, write K as

$$K \equiv K_1 + iK_2 = |K| e^{i\gamma} L^{-i\epsilon} \tag{14}$$

where by (6), L is the in-plane length quantity characterizing the specific interface crack problem when $a = 0$. The real angular quantity γ will be used as the measure of the loading combination. Then by (11), (13), and (14),

$$\mathcal{G} = q^{-2} \mathcal{G}_0 [|c|^2 + |d|^2 + 2R_e(cde^{2i\tilde{\gamma}})] \tag{15}$$

where

$$q = [(1-\beta^2)/(1+\alpha)]^{1/2} \tag{16}$$

and

$$\tilde{\gamma} = \gamma + \epsilon \ln(a/L). \tag{17}$$

When $\epsilon = 0$, the stress intensity factors, K_I and K_{II}, and $\mathcal{G}$ are *independent* of a. This is the case for similar moduli across the interface ($\alpha = \beta = 0$). By (4), ϵ is also zero whenever $\beta = 0$ regardless of the value of α. The oscillatory behavior of the interface crack fields and the a-dependence of $\mathcal{G}$ only appear when $\beta \neq 0$. A sensible approach to gaining insight into interfacial fracture behavior, while avoiding complications associated with the oscillatory singularity, would be to focus on material combinations with $\beta = 0$. Indeed, Hutchinson et al. (1987) tabulated strain values on α and β for six representative material combinations and found that β was quite small for most of the combinations. For example, *Mg*0 has a shear modulus more than four times that of A_u, yet this combination has $\alpha = .51$, $\beta = .011$, and $\epsilon = -.004$. In this paper, special attention is directed to material combinations with $\beta = 0$, but the role of β will also be examined.

When $\beta \neq 0$ and, therefore, $\epsilon \neq 0$, the interface crack with $a = 0$ suffers contact between the crack faces within some distance (usually exceedingly small) from the tip, as discussed recently by Rice (1987) and Anderson (1987), and as analyzed by Comninou (1977). Contact between crack faces is less likely

[1] In this paper the focus is on plane strain behavior. However, the results presented for the stress intensities are valid for plane stress as well when α and β are evaluated using plane stress formulas.

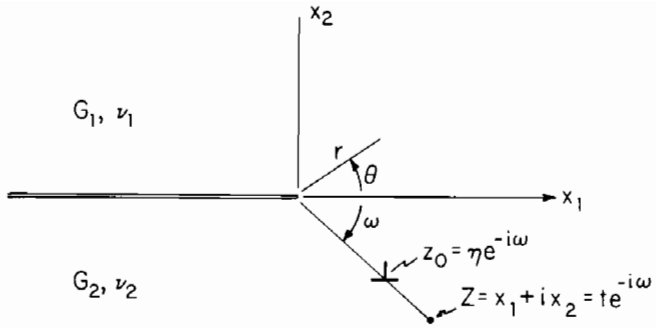

Fig. 3 Geometry and conventions for construction of integral equation

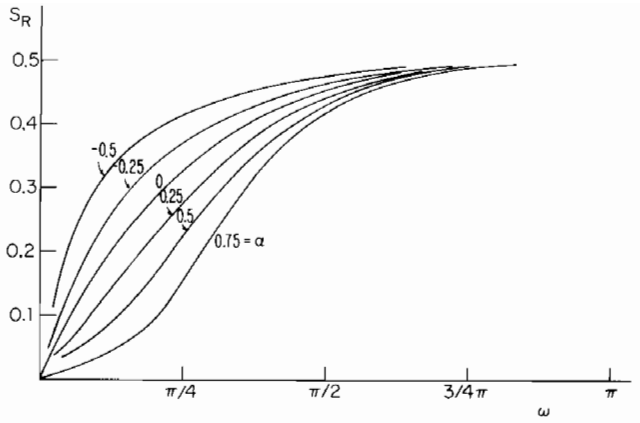

Fig. 4 Dependence of strength of singularity at kink, s, as a function of kink angle ω for various $\alpha(\beta = 0)$

for the kinked crack ($a>0$, $\omega>0$) loaded such that K_I and K_{II} are positive, since this will open up the crack at the kink. Nevertheless, contact will inevitably occur if $\epsilon\neq 0$ when a is sufficiently small compared to L.

The dependence of $\mathcal{G}$ on a for a given kink angle is sketched qualitatively in Fig. 2 as predicted by (15) when $\epsilon\neq 0$. When a/L becomes sufficiently small, $\mathcal{G}$ oscillates between a maximum $\mathcal{G}_U$ and a minimum $\mathcal{G}_L$, which are readily found to be

$$\mathcal{G}_U = q^{-2}\mathcal{G}_0[|c| + |d|]^2 \tag{18}$$

$$\mathcal{G}_L = q^{-2}\mathcal{G}_0[|c| - |d|]^2 \tag{19}$$

and which depend on K_1 and K_2 only through $\mathcal{G}_0$. For values of a/L outside the oscillatory range $\mathcal{G}$ approaches $\mathcal{G}^*$, given by (15), with $\tilde{\gamma} = \gamma$, i.e.,

$$\mathcal{G}^* = q^{-2}\mathcal{G}_0[|c|^2 + |d|^2 + 2R_e(cde^{2i\gamma})]. \tag{20}$$

Note that $\mathcal{G}^*$ coincides with $\mathcal{G}$ when $\epsilon = 0$. Contact between the crack faces will invalidate the prediction for $\mathcal{G}$ from (15) when a/L is in the range where oscillatory behavior occurs.

In presenting results for the energy release rate when $\epsilon\neq 0$, we will feature $\mathcal{G}^*$. From a physical standpoint, $\mathcal{G}^*$ should be relevant if there exist crack-like flaws emanating from the interface whose lengths are greater than the zone of contact. That is, $\mathcal{G}^*$ should be relevant for testing for kinking if the fracture process zone on the interface is large compared to the contact zone of the idealized elasticity solution. If it is not, then more attention must be paid to the a-dependence of $\mathcal{G}$ and to consideration of contact. In any case, $\mathcal{G}^*$ should play a prominent role in *necessary conditions* for a crack kinking out of an interface, because once nucleated, the kinked crack has an energy release rate which rapidly approaches $\mathcal{G}^*$ as it lengthens.

The final observation about the form of the solution concerns the behavior expected as $\omega\to 0$. When ω becomes small, the kinked segment parallels the interface and the solution approaches the solution obtained by Hutchinson et al. (1987) for a semi-infinite crack paralleling an interface a distance h below the interface. That solution has the property that $\mathcal{G} = \mathcal{G}_0$ and is given by

$$K_I + iK_{II} = qe^{i\phi}h^{i\epsilon}K \tag{21}$$

where ϕ is a real function of α and β which is tabulated by Hutchinson et al. (1987) and which is given approximately by $\phi = .158\alpha + .063\beta$ when α and β are small. In the present problem for small ω, h can be identified with $a\sin\omega \cong a\omega$ and (21) becomes

$$K_I + iK_{II} \cong qe^{i(\phi+\epsilon\ln\omega)}a^{i\epsilon}. \tag{22}$$

Thus, by comparing (8) and (22), one sees that for small ω

$$c\to qe^{i(\phi+\epsilon\ln\omega)}, \quad d\to 0, \quad \mathcal{G}\to\mathcal{G}_0. \tag{23}$$

2 Integral Equation and Solution Methods

The integral equation governing the solution to the kinked crack problem is constructed using a basic solution for an edge dislocation in material 2 interacting with a semi-infinite traction-free crack extending along the interface to the origin, as shown in Fig. 3. The dislocation is located at z_0 and its branch line extends parallel to the crack to $x_1\to-\infty$. Its radial and circumferential components of the Burgers vector along $\theta = -\omega$ are b_r and b_θ. The traction at z on $\theta = -\omega$ can be written as

$$\sigma_{\theta\theta}(t) + i\sigma_{r\theta}(t) = 2\tilde{B}e^{-i\omega}(t-\eta)^{-1} + BH_1(t,\eta) + \bar{B}H_2(t,\eta) \tag{24}$$

where

$$B = [G_2/(1-\nu_2)](b_r + ib_\theta)e^{-i\omega}/(4\pi i). \tag{25}$$

The functions H_1 and H_2 are specified in the Appendix. They are analytic at $t=\eta$, increase in proportion to $t^{-1/2}$ as $t\to 0$, and decrease in proportion to $\eta^{1/2}$ as $\eta\to 0$.

Denote the traction at z along $\theta = -\omega$ due to the interface crack tip field (3) by $\sigma^0_{\theta\theta}(t) + i\sigma^0_{r\theta}(t)$. This traction, which is also given in the Appendix, can be written as

$$\sigma^0_{\theta\theta}(t) + i\sigma^0_{r\theta}(t) = (Kh_1(t) + \bar{K}h_2(t))t^{-1/2}. \tag{26}$$

The functions h_1 and h_2 depend on ω and ϵ as well as t. When $\epsilon = 0$, h_1 and h_2 are independent of t.

The segment of the crack corresponding to $0\le t\le a$ is represented by a distribution of dislocations $B(\eta)$ chosen such that the net tractions resulting from (24) and (26) are zero on this line segment. Since the a-dependence of the solution is already known from (8), a is taken to be unity. The integral equation is then

$$2e^{-i\omega}\int_0^1 \tilde{B}(\eta)(t-\eta)^{-1}d\eta + \int_0^1 B(\eta)H_1(t,\eta)d\eta + \int_0^1 \bar{B}(\eta)H_2(t,\eta)d\eta = -(\sigma^0_{\theta\theta}(t) + i\sigma^0_{r\theta}(t)). \tag{27}$$

Similar formulations for other problems have been given by Bilby and Eshelby (1968), Rice (1968), and Hayashi and Nemat-Nasser (1968a,b).

Singularity at $t=1$. The dislocation density representing the kinked segment is proportional to $(1-t)^{-1/2}$ as $t\to 1$ and the stress intensity factors are given by

$$K_I + iK_{II} = (2\pi)^{3/2}e^{-i\omega}\lim_{t\to 1}\{(1-t)^{1/2}\bar{B}(t)\} \tag{28}$$

Singularity at $t=0$. A weaker singularity exists at the kink. The most singular stresses in the vicinity of the origin have the form $\sigma_{\alpha\beta}\sim r^{-s}\tilde{\sigma}_{ij}(\theta)$ where, in general, s is a complex number depending on ω, α, and β. Hein and Erdogan (1971) have derived the equation for s for the relevant bimaterial, wedge-shaped region. When $\beta = 0$, the imaginary part of s, s_1, is zero; the real part, s_R, is shown as a function of ω for several values

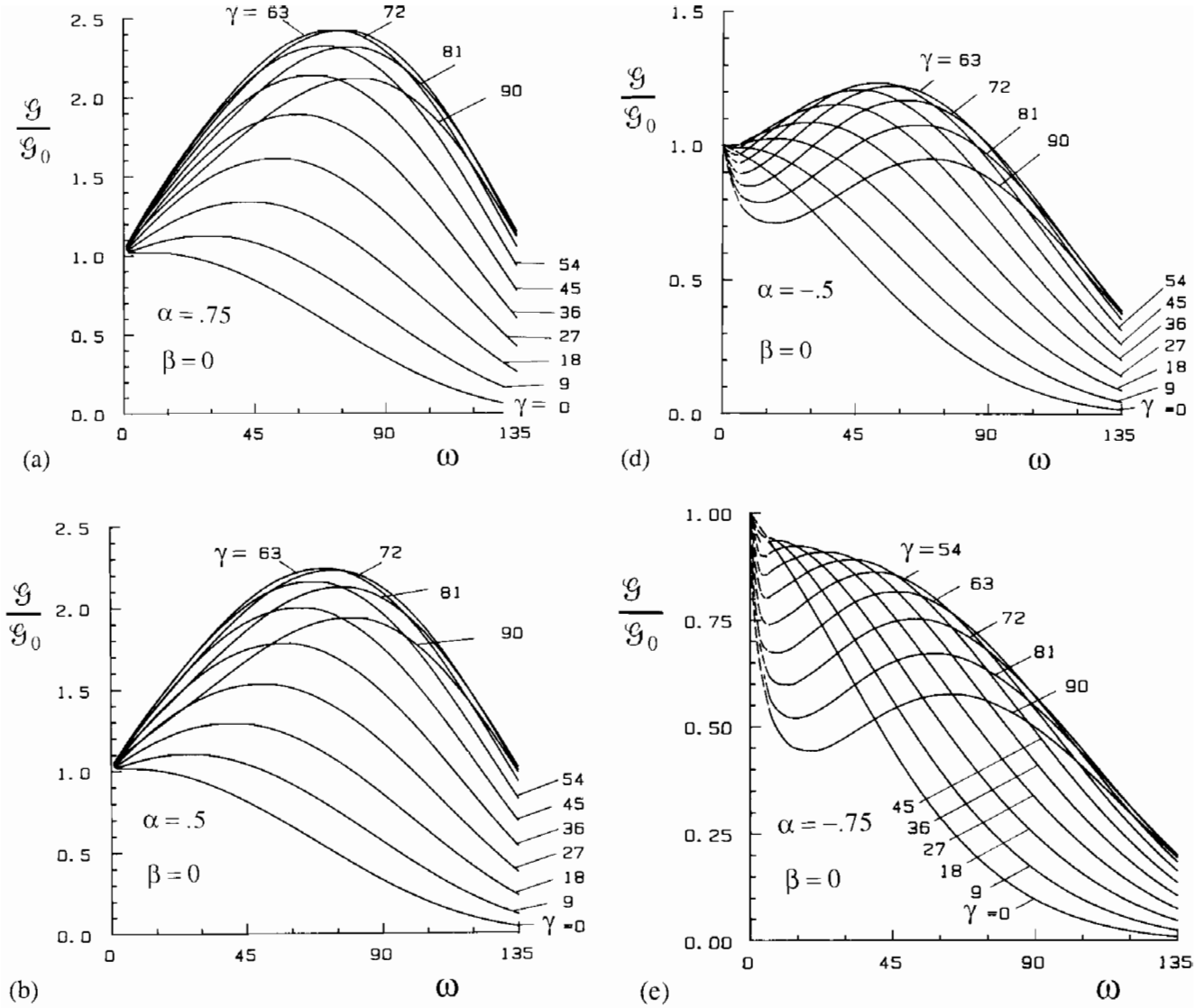

Fig. 5 Variation of $\mathcal{G}/\mathcal{G}_0$ with kink angle for loading combinations specified by $\gamma = \tan^{-1}(K_2/K_1)$ for various values of α, all with $\beta = 0$. The homogeneous case ($\alpha = \beta = 0$) is in (c).

of α in Fig. 4. When $\beta \neq 0$, s_1 is still zero over most of the range of ω except for ω greater than about $3\pi/4$ in most cases; the real part depends on ω in much the same way as displayed in Fig. 4. Thus, for essentially all cases of interest here, s is real and smaller than 1/2.

Solution Method #1. This method builds in the correct singularity of the dislocation distribution at each end of the interval with

$$B(\eta) = \eta^{-s}(1-\eta)^{-1/2}P(\eta) \tag{29}$$

where $P(\eta)$ is bounded on $0 \leq \eta \leq 1$. For an approximation with N unknown complex coefficients, C_j, P was represented by a polynomial of degree $N-1$ as

$$P(\eta) = \sum_{j=1}^{N} C_j \eta^{j-1}. \tag{30}$$

By substituting (29) and (30) in the integral equation (27) one obtains the equation

$$\sum_{j=1}^{N} \{C_j E_j(t) + \bar{C}_j F_j(t)\} = -(\sigma^0_{\theta\theta}(t) + i\sigma^0_{r\theta}(t)) \tag{31}$$

where the integral expressions for E_j and F_j are readily identified. To determine the N complex coefficients, (31) is satisfied at N points on the interval $0 < t < 1$; the set of Gauss-Legendre points were used once the interval had been mapped to $|t| \leq 1$. Some of the integrals making up the E_j and F_j must be evaluated numerically at each of the points t. Unusual care

Table 1 ($\omega = 45$ deg)

	Method #1		Method #2	
	$\alpha = 0$		$\beta = 0$	
N	$P_R(1)$	$P_m(1)$	$P_R(1)$	$P_m(1)$
4	0.05036	0.02135	0.04820	0.02046
8	0.05016	0.02113	0.04981	0.02112
10			0.04988	0.02112
12	0.05009	0.02106	0.04992	0.02111
16	0.05004	0.02104	0.04996	0.02109
20			0.04998	0.02107
40			0.05001	0.02103
	$\alpha = 0.56$		$\beta = 0.12$	
N	$P_R(1)$	$P_m(1)$	$P_R(1)$	$P_m(1)$
4	0.04268	0.01934	0.04279	0.01838
8	0.04207	0.01889	0.04216	0.01878
12	0.04204	0.01888	0.04208	0.01883
20			0.04204	0.01885
40			0.04202	0.01886
100			0.04201	0.01887

must be taken that these numerical integrations are performed accurately. It is this part of the computation which consumes the bulk of the computational effort. The polynomial representation (30) is equivalent to an expansion in any set of polynomials of degree $N-1$. The particular set (30) has certain advantages in reducing the computational effort involved in the numerical integrations.

Solution Method #2. This method is that used by Lo (1978) and Hayashi and Nemat-Nasser (1981a) which, in turn, follows the procedures developed by Erdogan and Gupta (1972). In our application of this method, s is taken to be $1/2$ in (29) and the condition $P(0) = 0$ is imposed. The recipes developed by Erdogan and Gupta and used by Lo can then be taken over directly even though the singularity at $t = 0$ is not strictly correct. At the Nth level of approximation, this method generates a system of algebraic equations for values of $P(\eta)$ at N Gauss-Chebychev points. The advantage of this method is that it requires far less numerical computation than Method #1 at the corresponding Nth level of approximation.

Table 1 compares results from the two methods for two examples at various levels of approximation. By (28) and (29), the stress intensity factors are given by

$$K_I + iK_{II} = (2\pi)^{3/2} e^{-i\omega} \overline{P(1)} \tag{32}$$

and Table 1 presents the real and imaginary parts of $P(1)$. The convergence of Method #1 is clearly faster than that of #2. Nevertheless, at corresponding levels of accuracy, Method #2 is still far more efficient than #1. The results presented in the following section were computed using Method #2 with $N = 40$. A number of test calculations indicated that the difference in the values of $P(1)$ computed with $N = 40$ and $N = 100$ was less than .1 percent except at small values of ω, as will be discussed later.

3 Numerical Results

Homogeneous Limit ($\alpha = \beta = 0$). The limiting case for crack kinking in a homogeneous material has been studied thoroughly in the literature, although considerable confusion has surrounded the problem because a number of early solutions were in error. Perhaps the most recent paper on the subject is that by Hayashi and Nemat-Nasser (1981a) which provides access to the literature. The results of Bilby, Cardew, and Howard (1977) derived using the method of Khrapkov (1971) and the results of Lo (1978) and Hayashi and Nemat-Nasser (1981a) are generally accepted to be correct, and our numerical results for this limit reproduced their results within the accuracy which could be inferred from their graphs and tables. All information can be derived from $c(\omega)$ and $d(\omega)$ in (8)-(10), and these coefficients are available in tabulated form in a limited-circulation companion report (He and Hutchinson, 1988). Our results agree within 1 percent with the equivalent set of tabulated coefficients included in the paper by Hayashi and Nemat-Nasser (1981a).

Plots of $\mathcal{G}/\mathcal{G}_0$ versus ω derived using (15) with the values of c and d are shown in Fig. 5(c) for a number of loading combinations as measured by $\gamma = \tan^{-1}(K_2/K_1)$. Since the crack has been taken to kink downward, the loading combinations which result in $K_1 > 0$ (i.e., an opening at the tip) *and* an opening at the kink will generally require $K_1 > 0$ and $\gamma \geq 0$. Results for the maximum energy release rate and its associated direction, together with the direction in which $K_{II} = 0$, will be presented later.

The approximation of Cotterell (1965), Vitek (1977), and Lawn and Wilshaw (1975) gives in the present notation

$$c = \frac{1}{2}\,(e^{-i\omega/2} + e^{-i3\omega/2}), \quad d = \frac{1}{4}\,(e^{-i\omega/2} - e^{i3\omega/2}). \tag{33}$$

Cotterell and Rice (1980) have shown that this approximation is asymptotically correct for small ω and is reasonably accurate for predicting K_I and K_{II} for ω as large as 45 deg or even 90 deg, depending on γ.

Bimaterial Problem With $\beta = 0$. As discussed in Section 1, cases with $\beta = 0$ and $\alpha \neq 0$ afford insight into interface problems without the added complication of oscillations, or contact, associated with nonzero ϵ. Roughly speaking, $\alpha > 0$ implies that material 1 is stiffer than material 2, and conversely. In the present paper the crack is always taken to kink downward into material 2 so that the relevant range of loading is restricted to $K_1 > 0$ and $\gamma > 0$ as mentioned earlier.

Values of $c(\omega)$ and $d(\omega)$ have been tabulated for various values of α and are available in He and Hutchinson (1988). Plots of $\mathcal{G}/\mathcal{G}_0$ versus ω for various γ are shown in Fig. 5 for $\alpha = .75, .5, 0, -.5$, and $-.75$. As noted in (23), $\mathcal{G} \to \mathcal{G}_0$ as $\omega \to 0$, and the numerical results for c and d were indeed in agreement with (23) for small ω. As long as α is positive the numerical method is accurate for ω as small as 1 deg. For negative values of α the numerical method became increasingly inaccurate as ω was decreased and results for ω less than about 5 deg could not be obtained accurately for the cases $\alpha = -.5$ and $-.75$. Thus, for $\omega < 5$ deg the curves in Fig. 5(d, e) have been interpolated to the limit $\mathcal{G} = \mathcal{G}_0$ for $\omega = 0$, and these sections of the curves have been dashed.

The qualitative features which emerge from the directional dependence of the energy release rate in Fig. 5 are the following: The more compliant is the material into which the crack kinks (i.e., the larger is α), the larger is the energy release rate, all other factors being equal. Conversely, if the lower material into which the crack kinks is relatively stiffer ($\alpha < 0$), then the energy release rate is reduced. These features are consistent with the role of moduli differences across an interface when a crack approaches the interface from within one of the two materials. When the differences are relatively large, the energy release rate for a crack kinking into the stiff material can be less than the interface release rate $\mathcal{G}_0$ for all combinations of loading, as can be seen in Fig. 5(e) for $\alpha = -.75$. This suggests that under conditions when the compliant material is tough and the stiff material and the interface are each relatively brittle with comparable toughnesses (as measured by a critical value of energy release rate), the crack will tend to be trapped in the interface for all loading combinations. If the stiff material is even less tough than the interface, the crack may leave the interface but not necessarily by kinking. For example, when $\alpha = -.75$ in Fig. 5(e), the largest energy release rates occur when ω is small approaching zero, suggesting that the crack may smoothly curve out of the interface. Such a path, however, would not necessarily satisfy $K_{II} \cong 0$. Some further discussion of these issues is given in the last section.

The direction $\hat{\omega}$ corresponding to the maximum energy release rate (i.e., where $d\mathcal{G}/d\omega = 0$ or at $\omega = 0$, whichever gives the larger $\mathcal{G}$) is displayed as a function of the loading angle γ for various α in Fig. 6. For positive α, when the crack enters the more compliant material, $\hat{\omega}$ increases smoothly as γ increases from 0 deg to 90 deg. Note that even when $K_2 = 0$ (i.e., $\gamma = 0$), the direction of maximum energy release rate is a finite angle into material 2 when $\alpha > 0$. For negative α there is a range of γ in the vicinity of $\gamma = 0$ for which the maximum occurs at $\omega = 0$. In addition, for sufficiently negative α the maximum of $\mathcal{G}$ also occurs at $\omega = 0$ when γ is in the vicinity of 90 deg, as can be seen in Fig. 5. For α, more negative than $-.67$, the maximum occurs at $\omega = 0$ for all γ.

The direction $\tilde{\omega}$ corresponding to $K_{II} = 0$ is sometimes suggested as an alternative to $\hat{\omega}$ as the kink direction. A comparison between $\tilde{\omega}$ and $\hat{\omega}$ is shown in Fig. 7 for $\alpha = 0$ and $\pm .5$. In the homogeneous case when $\alpha = 0$, the difference between $\tilde{\omega}$ and $\hat{\omega}$ is less than 1 deg for nearly all γ except near $\gamma = \pi/2$ where it becomes about 2 deg. (Apparently, a numerical comparison between these two directions has not previously been reported for the homogeneous case.) The difference between the two directions is also very minor for $\alpha = \pm .5$. It would be virtually impossible to distinguish between these directions using experimental observation of kinked cracks. For more negative values of α than $-.5$, the range of γ in which $\mathcal{G}_{max}$ occurs at $\hat{\omega} = 0$ becomes significant, while $K_{II} = 0$ at values of ω near the local maximum of $\mathcal{G}$ (see Fig. 5(*e*)) which occurs for ω between about 45 deg and 60 deg depending on γ. In this range of γ, $\tilde{\omega}$ and $\hat{\omega}$ are significantly different.

Bimaterial Problem With $\beta \neq 0$. Values of $c(\omega)$ and $d(\omega)$ have also been tabulated in He and Hutchinson (1988) for various pairs of α and β. The calculated values are in accord with the limits for small ω indicated in (23) although for values ω less than some value between 1 deg and 5 deg, depending on α and β, the computational procedure begins to become inaccurate.

As discussed in connection with (15), $\mathcal{G}$ is not independent of a when $\epsilon \neq 0$, but $\mathcal{G}$ approaches $\mathcal{G}^*$ for all but very small a.

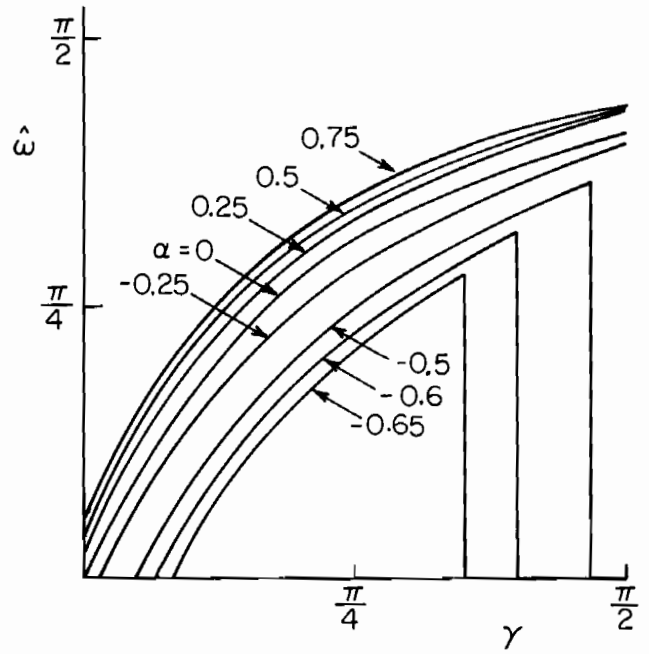

Fig. 6 Kinking angle $\hat{\omega}$ corresponding to maximum energy release rate as a function of the loading combination $\gamma = \tan^{-1}(K_2/K_1)$, in each case for $\beta = 0$

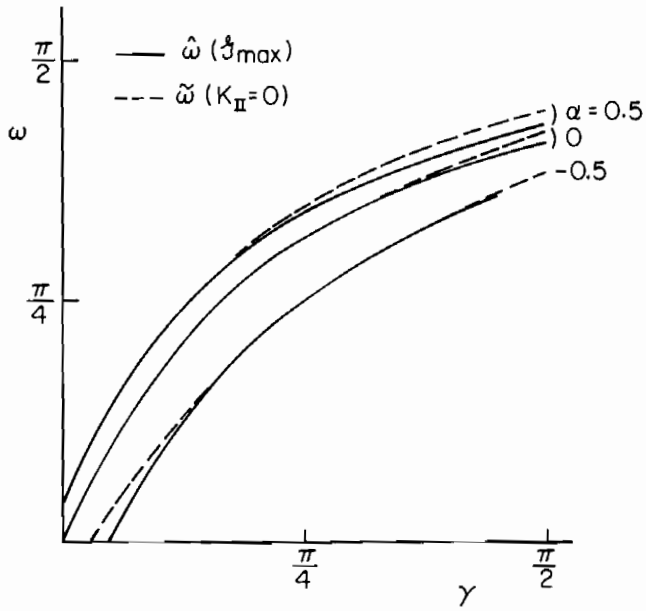

Fig. 7 Kinking angle associated with $K_{II} = 0$, $\tilde{\omega}$, as a function of γ compared with kinking angle associated with maximum energy release rate, $\hat{\omega}$, in each case for $\beta = 0$

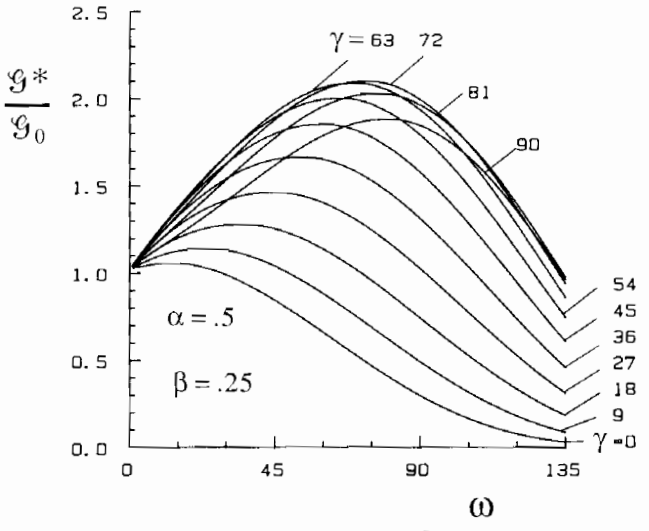

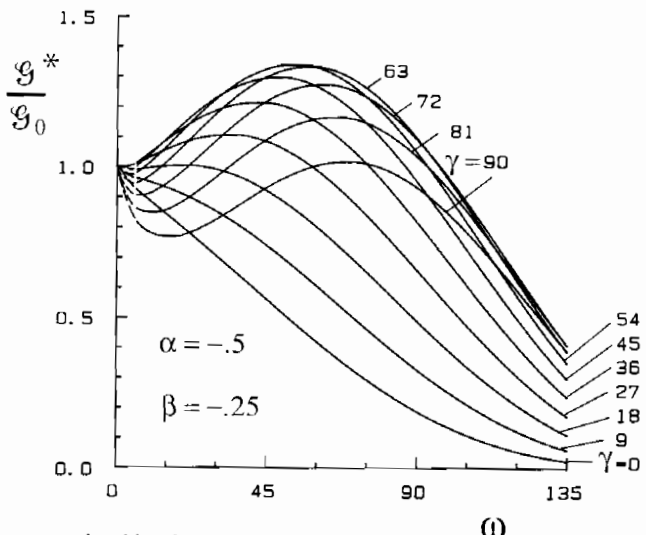

Fig. 8 $\mathcal{G}^*/\mathcal{G}_0$ versus ω for two cases in which $\beta \neq 0$

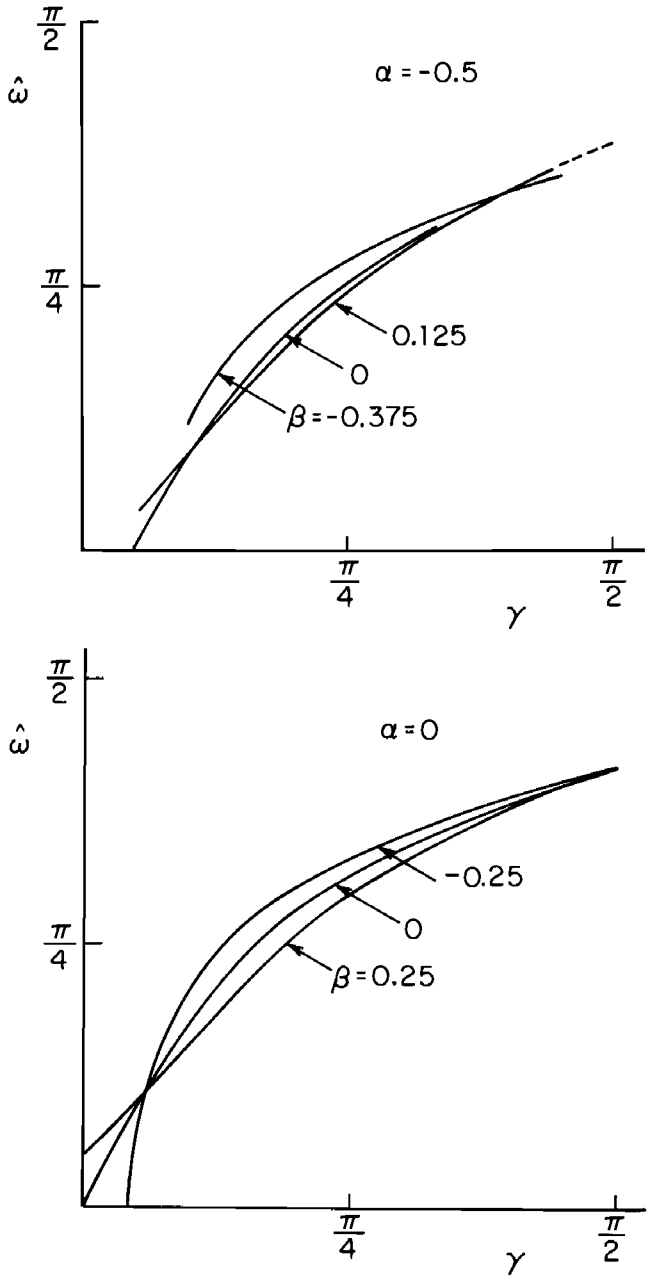

Fig. 9 Kinking angle $\hat{\omega}$ associated with maximum value of $\mathcal{G}^*$

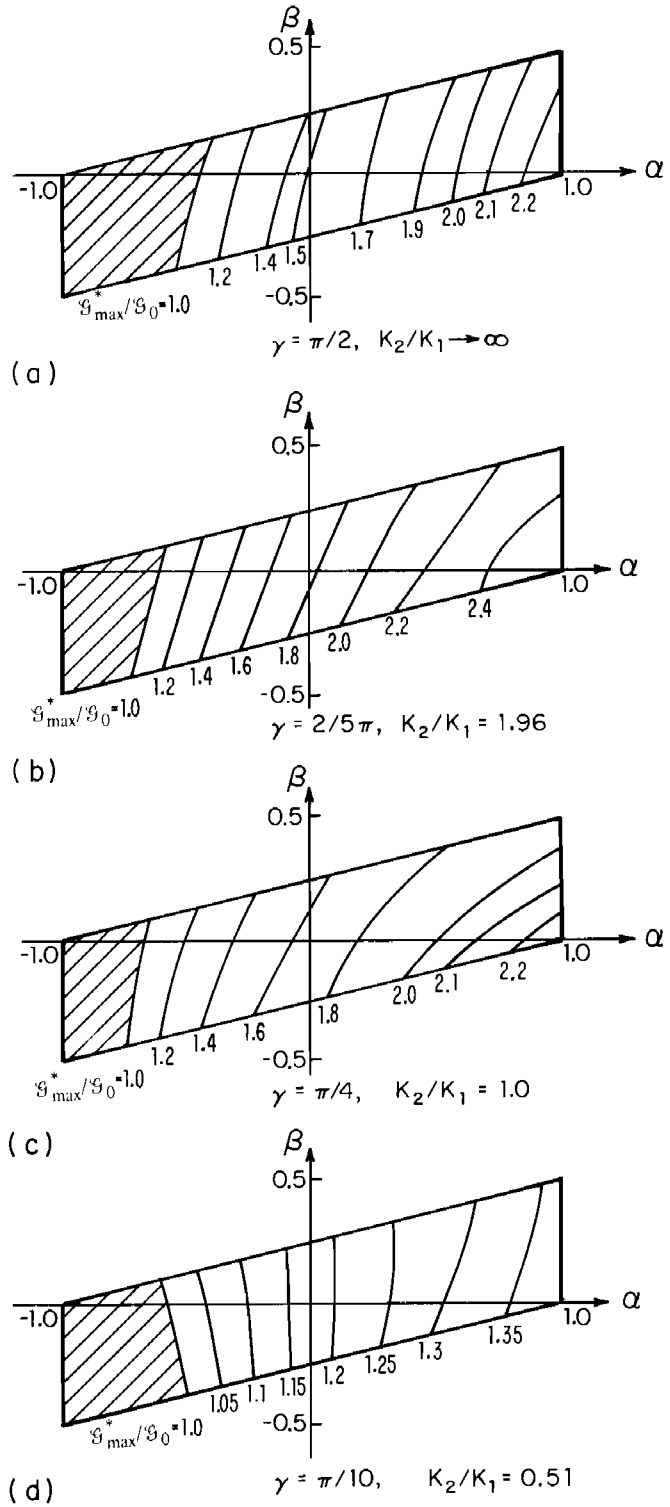

Fig. 10 Contour plots of the maximum value of $\mathcal{G}^*/\mathcal{G}_0$ as a function of α and β for four loading combinations specified by γ. The shaded regions correspond to $(\mathcal{G}^*/\mathcal{G}_0)_{max} = 1$ with $\hat{\omega} - 0$.

Plots of $\mathcal{G}^*/\mathcal{G}_0$ as a function of ω are shown in Fig. 8 for (α = .5, β = .25) and (α = −.5, β = −.25). Although the β-values in these examples are quite large, the curves are quite similar to the curves in Fig. 5 with the same values of α and with β = 0. Curves of $\hat{\omega}$ associated with the maximum value of $\mathcal{G}^*$ are shown versus γ in Fig. 9. The effect of β on this variable appears to be relatively weak.

Contour plots of maximum values of $\mathcal{G}^*/\mathcal{G}_0$ are shown in Fig. 10 where α and β are coordinates whose range shown is restricted to non-negative values of the Poisson's ratios, ν_1 and ν_2. Each of the four plots is associated with a given loading combination measured by γ. The cross-hatched areas coincided with those pairs of α and β for which the maximum value of $\mathcal{G}^*$ is $\mathcal{G}_0$ with $\hat{\omega}$ = 0. Note that $\mathcal{G}^*_{max}/\mathcal{G}_0$ varies by roughly a factor of 2 for α ranging from 1 to −1. These plots also reveal that the dependence of $\mathcal{G}^*_{max}$ on β is not particularly strong, especially in the range $|\beta| < .1$.

The only other paper on cracks kinking out of a bimaterial interface appears to be that of Hayashi and Nemat-Nasser (1981b). These authors consider a very special crack geometry and account for crack surface contact.

4 Concluding Remarks

The results for the kinked crack can be used to assess whether an interface crack will propagate in the interface or whether it will kink out of the interface. The simplest ap-

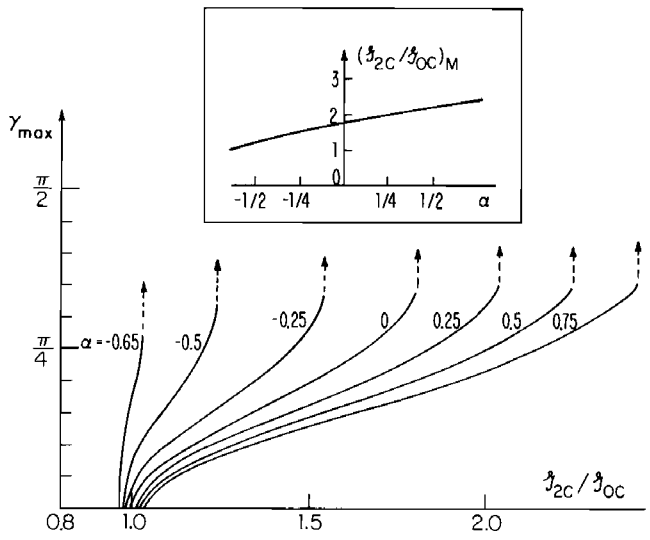

Fig. 11 For loading combinations $\gamma = \tan^{-1}(K_2/K_1)$ satisfying $0 \le \gamma \le \gamma_{max}$ the crack will not kink out of the interface into material 2. Assuming a propagation criterion based on maximum energy release rate, the dependence of γ_{max} on the ratio of material 2 toughness to interface toughness is shown for various α, all with $\beta = 0$. The insert figure shows the minimum value of this toughness ratio needed to ensure that the crack will not kink into material 2 for all loading combinations.

proach is to assume that the condition for propagation in the interface is $\mathcal{G}_0 = \mathcal{G}_{0c}$ and that for propagation in material 2 is $\mathcal{G} = \mathcal{G}_{2c}$. If $\mathcal{G}_{2c}$ is sufficiently large, compared to $\mathcal{G}_{0c}$, the crack will never kink into material 2. When $\mathcal{G}_{2c}$ is comparable to $\mathcal{G}_{0c}$ there will still be a loading range, i.e., $0 \le \gamma < \gamma_{max}$, such that the crack stays in the interface, while for $\gamma > \gamma_{max}$, the interface crack will kink into material 2. Figure 11 displays the dependence of γ_{max} on $\mathcal{G}_{2c}/\mathcal{G}_{0c}$ for various α-values, all with $\beta = 0$. When material 2 is the more compliant material $\mathcal{G}_{2c}$ must be greater than the interface toughness $\mathcal{G}_{0c}$ by as much as 2.5 (for $\alpha = .75$) if the crack is to stay in the interface for all γ. On the other hand, when material 2 is relatively stiff ($\alpha = -.65$), the crack will stay in the interface as long as $\mathcal{G}_{2c} \cong \mathcal{G}_{0c}$. The plot in the insert in Fig. 11 gives the *minimum value* of the toughness ratio, $(\mathcal{G}_{2c}/\mathcal{G}_{0c})_M$, needed to ensure that the crack will not leave the interface and propagate in material 2 for *all* combinations of loading.

A similar analysis can be carried out when $\mathcal{G}_{0c}$ depends on γ. This can be expected when the fractured interface has some roughness, with $\mathcal{G}_{0c}$ increasing with γ. Curves similar to those in Fig. 11 can be plotted from the basic results in Section 3. The important point is that the level of $\mathcal{G}_{2c}$ required to prevent kinking out of the interface will depend on the interface toughness $\mathcal{G}_{0c}$ at the loading angle γ applied.

When there is no dissimilarity in the elastic properties of the materials across the interface, the directions of kinking associated with the maximum energy release rate and with $K_{II} = 0$ are virtually the same (cf. Fig. 7). This is also true when the crack kinks into the more compliant material ($\alpha > 0$), at least when $\beta = 0$. However, when the crack kinks into a material 2 which is substantially stiffer than material 1, there exist ranges of loading where the maximum energy release rate occurs at small kink angles while the kink angle associated with $K_{II} = 0$ is around 45 deg or larger. When $\alpha < -.67$ (with $\beta = 0$) the direction $\bar{\omega}$ associated with $K_{II} = 0$ is quite different from the direction of maximum energy release rate ($\hat{\omega} \cong 0$) for all loading combinations. It is an open question as to the criterion for crack kinking out of an interface when $\hat{\omega}$ and $\bar{\omega}$ differ considerably. When the crack has penetrated well into material 2 a criterion based on $K_{II} = 0$ is expected to hold. A choice of criterion for the initial kinking step will have to be guided by experiment.

Pathological crack tip behavior associated with nonzero β (i.e., nonzero ϵ) has stood in the way of the development of an interfacial fracture mechanics for some years. This is in spite of the fact that there does not appear to be any compelling experimental evidence that the unusual behavior associated with nonzero β is essential to interfacial fracture phenomena. As a way to break the impasse, a tentative proposal put forward in the body of the paper is that the role of β be downplayed by arbitrarily taking $\beta = 0$ in the use of analytical results to interpret tests and make predictions, especially when β is small anyway. Such an approach seems sensible where the primary fracture variables of interest depend weakly on β, as is the case for most quantities examined in this paper. Obviously, a continual monitoring for any possible essential role of β should go on if this proposal is adopted.

Acknowledgments

This work was supported in part by DARPA University Research Initiative (Subagreement P.O. #VB38639-0 with the University of California, Santa Barbara, ONR Prime Contract N00014-86-K-0753) and by the Division of Applied Sciences, Harvard University.

References

Anderson, P. A., 1988, "Small Scale Contact Conditions for the Linear-Elastic Interface Crack," ASME JOURNAL OF APPLIED MECHANICS, Vol. 55, pp. 814-817.

Bilby, B. A., Cardew, G. E., and Howard, I. C., 1977, "Stress Intensity Factors at the Tip of a Kinked and Forked Cracks," *Fracture, 1977*, Vol. 3, University of Waterloo Press, p. 197.

Bilby, B., and Eshelby, J. D., 1968, "Dislocations and the Theory of Fracture," *Fracture, and Advanced Treatise*, Vol. I, H. Liebowitz, ed., Academic Press, New York, pp. 99-182.

Comninou, M., 1977, "The Interface Crack," ASME JOURNAL OF APPLIED MECHANICS, Vol. 44, pp. 631-636.

Cotterell, B., 1965, "On Brittle Fracture Paths," *Int. J. Fracture Mech.*, Vol. 1, pp. 96-103.

Cotterell, B., and Rice, J. R., 1980, "Slightly Curved or Kinked Cracks," *Int. J. Fracture*, Vol. 16, pp. 155-169.

Dundurs, J., 1969, "Edge-bonded Dissimilar Orthogonal Elastic Wedges," ASME JOURNAL OF APPLIED MECHANICS, Vol. 36, pp. 650-652.

England, A. H., 1965, "A Crack Between Dissimilar Media," ASME JOURNAL OF APPLIED MECHANICS, Vol. 32, pp. 400-402.

Erdogan, A. H., 1965, "Stress Distribution in Bonded Dissimilar Materials with Cracks," ASME JOURNAL OF APPLIED MECHANICS, Vol. 32, pp. 403-410.

Erdogan, F., and Gupta, G. D., 1972, "On the Numerical Solution of Singular Integral Equations," *Quarterly of Appl. Math.*, Vol. 29, pp. 525-534.

Hayashi, K., and Nemat-Nasser, S., 1981a, "Energy-Release Rate and Crack Kinking under Combined Loading," ASME JOURNAL OF APPLIED MECHANICS, Vol. 48, pp. 520-524.

Hayashi, K., and Nemat-Nasser, S., 1981b, "On Branched, Interface Cracks," ASME JOURNAL OF APPLIED MECHANICS, Vol. 48, pp. 529-533.

He, M-Y., and Hutchinson, J. W., 1988, "Kinking of a Crack Out of an Interface: Tabulated Solution Coefficients," Harvard University Report MECH-113A (available for a limited period from Marion Remillard, Pierce Hall 314, Division of Applied Sciences, Harvard University, Cambridge, MA 02138).

Hein, V. L., and Erdogan, F., 1971, "Stress Singularities in a Two-Material Wedge," *Int. J. Fracture Mech.*, Vol. 7, pp. 317-330.

Hutchinson, J. W., Mear, M., and Rice, J. R., 1987, "Crack Paralleling an Interface Between Dissimilar Materials," ASME JOURNAL OF APPLIED MECHANICS, Vol. 54, pp. 828-832.

Khrapkov, A. A., 1971, "The First Basic Problem for a Notch at the Apex of an Infinite Wedge," translated by I. Sneddon, *Int. J. Fracture Mech.*, pp. 373-382.

Lawn, B. R., and Wilshaw, T. R., 1975, *Fracture of Brittle Solids*, Cambridge University Press.

Lo, K. K., 1978, "Analysis of Branched Cracks," ASME JOURNAL OF APPLIED MECHANICS, Vol. 45, pp. 792-802.

Malyshev, B. M., and Salganik, R. L., 1965, "The Strength of Adhesive Joints Using the Theory of Cracks," *Int. J. Fracture Mech.*, Vol. 1, pp. 114-118.

Rice, J. R., 1968, "Mathematical Analysis in the Mechanics of Fracture," *Fracture, an Advanced Treatise*, Vol. II, H. Liebowitz, ed., Academic Press, New York, pp. 191-311.

Rice, J. R., 1988, "Elastic Fracture Mechanics concepts for Interfacial Cracks" ASME JOURNAL OF APPLIED MECHANICS, Vol. 55, pp. 98-103.

Rice, J. R., and Sih, G. C., 1965, "Plane Problems of Cracks in Dissimilar Media," ASME JOURNAL OF APPLIED MECHANICS, Vol. 32, pp. 418-423.

APPENDIX

The basic solution for an edge dislocation at z_0 ($z_0 = \eta e^{-i\omega}$) in material 2 interacting with a semi-infinite, traction-free crack extending along the interface to the origin (Fig. 3) was obtained by using complex variable methods. If the traction on the radial line through z ($z = te^{-i\omega}$) is written as (24), the functions H_1 and H_2 are given by

$$\begin{aligned} H_1(t,\eta) &= H_{10}(t,\eta) + H_{11}(t,\eta) \\ H_2(t,\eta) &= H_{20}(t,\eta) + H_{21}(t,\eta) \end{aligned} \tag{A1}$$

where

$$H_{10} = -\delta\left(\frac{1}{z-\bar{z}_0} + \frac{(\bar{z}_0 - z_0)}{(z-z_0)^2} + e^{-2i\omega}\,\frac{(\bar{z}_0 - \bar{z})}{(z-\bar{z}_0)^2}\right)$$

$$H_{20} = -\delta\left(\frac{1}{\bar{z}-z_0} + \frac{(z_0-\bar{z}_0)}{(z-\bar{z}_0)^2} + e^{-2i\omega}\frac{(z_0-\bar{z}_0)(z+\bar{z}_0-2\bar{z})}{(z-\bar{z}_0)^3}\right) - \frac{\lambda}{z-\bar{z}_0}\,e^{-2i\omega} \tag{A2}$$

and

$$H_{11} = -(1+\alpha)(1-\beta)\,\mathcal{L}\left[\frac{F(z,z_0)}{1-\beta} + \frac{F(z,\bar{z}_0)}{1+\beta}\right]$$

$$H_{21} = -(1+\alpha)(1-\beta)\,\mathcal{L}\left[\frac{z_0-\bar{z}_0}{1+\beta} + \frac{\partial}{\partial \bar{z}_0}\,F(z,\bar{z}_0)\right].$$

The functions H_{10} and H_{20} are for a dislocation below the bimaterial interface without the crack. The functions H_{11} and H_{21} are the additional terms to satisfy the traction-free condition on the semi-infinite crack. In the above

$$\delta = \frac{\beta-\alpha}{1+\beta}\,, \quad \lambda = \frac{\alpha+\beta}{\beta-1} \tag{A3}$$

and

$$\mathcal{L}(\phi(z)) = \phi(z) + \overline{\phi(z)} + e^{-2i\omega}\left[(\bar{z}-z)\phi'(z) + \frac{(1-\beta)}{(1+\beta)}\,\bar{\phi}(z) - \phi(z)\right]$$

$$F(z,z_0) = \frac{1}{2}\left[1 - \left(\frac{z_0}{z}\right)^{1/2+i\epsilon}\right]/(z-z_0). \tag{A4}$$

The formula for $\sigma^0_{\theta\theta}(t) + i\sigma^0_{r\theta}(t)$ in (26) is

$$\sigma^0_{\theta\theta} + i\sigma^0_{r\theta} = \phi_0'(z) + \overline{\phi_0'(z)} + e^{-2i\omega}[\bar{z}\phi_0''(z) + \chi_0'(z)] \tag{A5}$$

where

$$\phi_0'(z) = \frac{1}{2\sqrt{2\pi}\,\cosh\,\pi\epsilon}\,e^{-\epsilon\pi}\bar{K}z^{-(1/2+i\epsilon)}$$

$$\chi_0'(z) = \frac{1}{2\sqrt{2\pi}\,\cosh\,\pi\epsilon}\left[e^{\epsilon\pi}Kz^{-1/2+i\epsilon} - e^{-\epsilon\pi}\left(\frac{1}{2} - i\epsilon\right)\bar{K}z^{-(1/2+i\epsilon)}\right]. \tag{A6}$$